Direct HRTEM Observation of Ultrathin Freestanding Ionic Liquid Film on Carbon Nanotube Grid

Shimou Chen,[†] Keita Kobayashi,[‡] Ryo Kitaura,[†] Yasumitsu Miyata,[†] and Hisanori Shinohara[†,*]

[†]Department of Chemistry and Institute for Advanced Research, Nagoya University, Nagoya, 464-8602, Japan, and [‡]Nanotube Research Center, National Institute of Advanced Industrial Science and Technology, Tsukuba 305-8565, Japan

ABSTRACT Direct imaging of liquids by electron microscopy has been extremely difficult due to their high volatility. Ionic liquids are a unique liquid material with almost zero vapor pressure, which allows us to characterize them under high-vacuum conditions. Here we report the first direct observation of the microstructure and phase behavior of an imidazolium-based room-temperature ionic liquid by high-resolution transmission electron microscopy with the aid of a special carbon nanotube network, which is able to support a freestanding ultrathin ionic liquid film on its nanosized holes. It was found that the existence of cluster structures is one of the intrinsic properties of the ionic liquid in its whole liquid phase range. Furthermore, the size and mobility of the clusters play an important role during phase transition of the ionic liquid. We show that the direct HRTEM imaging on freestanding liquid film is a powerful technique to obtain insight into the structure of ionic liquids and their phase behavior. The present study can provide an important starting point for more sophisticated structural studies on the microstructure of liquidus materials.

KEYWORDS: ionic liquid · cluster · electron microscopy · freestanding liquid film · phase transition

The microscale/nanoscale structure of liquids is an important topic and has attracted much attention due to their relevance in solvent properties, reaction dynamics, crystal engineering, material synthesis, and chemical processes. Liquid cluster models have been proposed more than a century ago and provided fundamental ideas for understanding the bulk liquid. Clusters/aggregates in water,[1−4] organic solvents,[5,6] inert gases,[7] and liquid metals[8] have been confirmed by various spectroscopic analyses as well as theoretical calculations. Most of the experimental evidence, which supports this kind of spatial-heterogeneity property, has been obtained indirectly by capturing the structures in the gas phase or solid state,[1,6] entrapping liquids inside inorganic/organic matrices,[4,7] and bombing liquids by high-energy particles.[9] However, direct microscopic evidence of this territory remains unexplored.

High-resolution transmission electron microscopy (HRTEM) is a powerful technique for probing the structure of materials on the nanometer and sub-nanometer scale. Unfortunately, normal molecular liquid samples preclude any direct HRTEM observations due to their volatilities. Furthermore, to increase the spatial resolution, an ultrathin film sample is required for HRTEM observations. Direct observation of a freestanding ultrathin film of liquid is an important challenge in HRTEM studies because it is free from the interface of the support material (substrate) or container of the liquid sample.[10,11] This surely can provide real views of the liquid structure at nanometer scale.

Ionic liquids are considered as promising solvents and functional materials because of their unique properties such as extremely low volatility, nonflammability, high stability, and electroconductivity.[12−15] The extremely low vapor pressure and high stability, in particular, nicely match the requirements of HRTEM observation.[16] A molecular-based understanding of structure and properties of ionic liquids has so far been a great challenge because of the unusual complexity of their intermolecular interactions. Some well-established rules and correlations for assessing the properties of molecular liquids are not easily transferred to ionic liquids.[17] One may attribute ionic liquids to a microheterogeneous structure based on the results of scattering experiments and simulations.[18−20] However, there is still no direct evidence to support this speculation. Many of these important issues and controversies could be solved or reconsidered by directly observing microstructures of ionic liquids by HRTEM.

To observe a freestanding liquid film by HRTEM, we need a special supporting film that is highly conductive, robust, and most importantly nanoholey. The idea was

* Address correspondence to noris@nagoya-u.jp.

Received for review March 16, 2011 and accepted May 19, 2011.

Published online May 19, 2011
10.1021/nn2009968

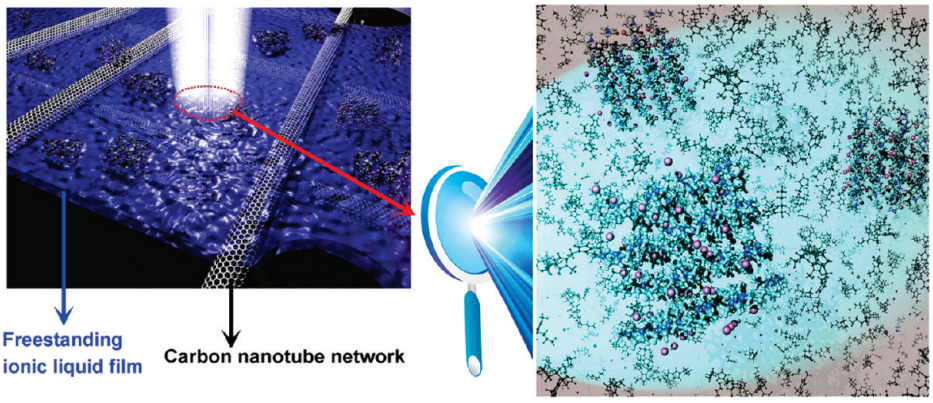

Figure 1. Schematic diagram for the HRTEM observation of a freestanding ionic liquid film on a carbon nanotube grid.

enlightened by the fact that a fishing net can support water films on its millimeter-sized holes. If we use the nanosized hole to support a liquid film, the thickness of the freestanding liquid could be reduced to nanometer scale (Supporting Figure S1). In this study, a special HRTEM grid made by cross-stacking ultrathin superaligned carbon nanotube films onto the surface of copper grids was employed for TEM observations.[21] The carbon nanotube grid has a large number of nanosized holes (Supporting Figure S2). We have incorporated this special carbon nanotube network to support the thin film of ionic liquids and realized the direct observation of a freestanding ionic liquid film by HRTEM under nanoscale resolution (Figure 1).

RESULTS AND DISCUSSION

A prototype ionic liquid, 1-butyl-3-methylimidazolium iodide (bmiml), was chosen as a sample to achieve a high resolution and contrast for HRTEM imaging. As shown in Figure 2a, the EDX analysis shows that the thin film is composed of bmiml ionic liquid (Figure 2c). At room temperature, the fluctuation of image contrasts and drift of the film were observed, suggesting that the bmiml is in liquid state. Even so, HRTEM images clearly show crystalline clusters in the liquid film (Figure 2b). The HRTEM micrographs reveal that the clusters exhibit various crystalline orientations with a typical size of 2 to 5 nm across (Figure 2d). The clusters exist randomly in the holes of the carbon nanotube network, which preclude the possibility of a carbon nanotube surface induced ordering mechanism.[22]

To the best of our knowledge, the "knock-on damage" threshold for ionic liquids has not been studied so far. In this study, we used two different microscopes to observe the bmiml thin film: (1) a JEOL JEM-2010F/UHR equipped with a Cs corrector operating at 120 kV; (2) a JEOL JEM 2100F/HR microscope operating at 80 kV. We could easily observe the cluster structures in the bmiml films on each microscope, implying a higher radiation stability of the bmiml ionic liquid as compared with the normal organic compounds. More importantly, the electron beam radiation effects on the

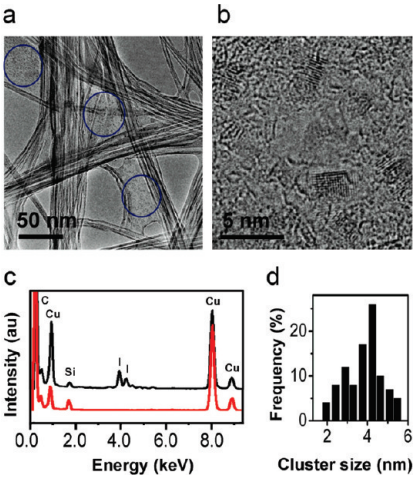

Figure 2. HRTEM images of the freestanding bmiml ionic liquid thin films. (a) TEM image of the bmiml ionic liquid thin film supported by the nanosized holes on a carbon nanotube network. The blue circles mark the location of the freestanding bmiml thin film on the grid. (b) High-resolution TEM image showing the existence of well-ordered clusters in the bmiml thin film. (c) Energy dispersive X-ray spectra from the bmiml thin film (black) and carbon nanotube based TEM grid (red). The observed Si and Cu signals are from the carbon nanotube network and sample holder. (d) Histogram of the cluster size distribution at 25 °C, obtained from measurements of 80 clusters.

films during TEM imaging were carefully studied. As shown in Figure 3, by exposing the bmiml thin film to continuous electron beam irradiation with an accelerating voltage of 120 kV, the percentage of cluster area in the film was plotted as a function of electron dose. It was found that the radiation effect results in an increasing of the ratio of cluster area (the reason is presented in the Supporting Information, section 3). More importantly, when the graph is extrapolated to zero radiation dose, all three line plots suggested the existence of a considerably large cluster area, which is completely not dependent on the electron beam radiation, which suggested the inherent existence of the clusters in pristine ionic liquid. It should be mentioned that the bmiml clusters show a high radiation stability; they can be observed until the thin film is

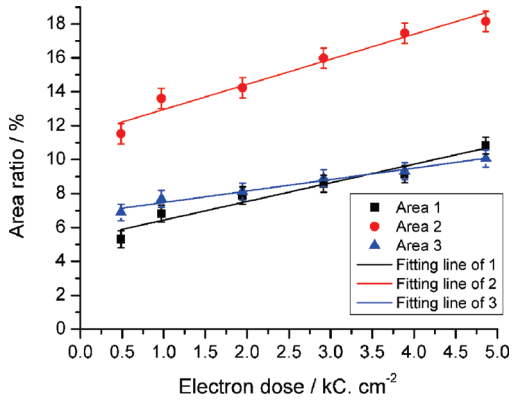

Figure 3. Percentage of cluster-occupied area in the HRTEM images of bmimI thin film as a function of radiation dose. Three different areas (900 nm^2 for each) were investigated and 6 data points were calculated from the time-dependent TEM observations for each area. The irradiation times are 1, 2, 4, 6, 8, and 10 min, corresponding to the absorbed electron dose of 0.486, 0.972, 1.944, 2.916, 3.888, and 4.860 kC·cm^{-2}. Error bars are the standard deviations. The TEM experiments were conducted under a constant 80 kV accelerating voltage at 25 °C.

broken under prolonged electron beam radiation (Figure S5 and Movie S2).

We also studied the thermal stability of bmimI clusters by using the *in situ* heating system in our TEM. A series of TEM images were taken of a specific area under different temperatures (Supporting Information, Figure S6). With increasing temperature (we focused on a specific area of the bmimI film at 25, 160, 210, 260, 300, and 340 °C, respectively), the area ratio of clusters:phase decreased. However, there were still many clusters when the temperature reached 340 °C (further increase of the temperature will lead to the dissociation of the bmimI film by thermal decomposition). This implies that the existence of cluster structures (or aggregates) is one of the intrinsic properties of the bmimI ionic liquid in its whole liquid phase range. Furthermore, when we examined the radiation stability of the bmimI cluster at 300 °C, with the aid of continuous electron beam radiation, we finally observed a step-by-step dissociation of two isolated bmimI clusters upon irradiation (arrows in Figure 4; a motion picture is shown in Movie S3).

We noticed that the ordered clusters are more frequently observed in the relatively thin bmimI film (Supporting Figure S12), indicating that the ultrathin film is a key factor for the detection of clusters due to the extremely small size of the clusters. Although we do not know exactly the thickness of the bmimI film, we have found that the typical freestanding bmimI thin film (prepared from bmimI solution at 1.0 wt %) is often seen to be mounted inside the holes of the carbon nanotube network, resulting in a protrusion of the surrounding carbon nanotubes (Figure 2a). The thickness of the bmimI film should, therefore, be of the same scale or less than that of the height of its supporting tubes. Since the diameter of the carbon nanotubes used is within 10−20 nm, the typical thickness of the freestanding bmimI film should be tens of nanometers.

In order to estimate the thickness of a typical bmimI thin film and check the TEM contrast of the clusters in liquid films, we carried out a TEM image simulation by the standard TEM simulation algorithm.[23] For the structural models, a bmimI cluster (derived from the crystal structure of bmimI[24]) containing 108 ion pairs was put in the center of a bmimI thin film with a thickness of 5, 10, 20, 30, and 40 nm, respectively. In a typical thin film construction process, first, the bmimI cluster was centered in a 5 nm × 5 nm × 5 nm cubic box (the thickness is 5 nm in this case), with the ions positioned on lattice positions. Second, the initial cluster was solvated in 287 bmimI molecules to mimic the surrounding liquid state of bmimI. This solvation process was performed by molecular dynamics program Gromacs 3.3. The final density of the liquid film is near the bulk bmimI density, 1.4 g/cm^3.

The structural models and corresponding simulated images are shown in Figure 5. Compared with the experimental TEM images, the simulated images of clusters show similar contrast when the thickness of the liquid film is 20 or 30 nm. However, the clusters cannot be detected when the thickness is equal to 40 nm, indicating the film thickness plays a key role in the imaging of the clusters by TEM. This is also supported by our *in situ* TEM observation on the thickness transformations of a bmimI thin film upon continuous electron beam radiation (Supporting Information, Figure S4 and Movie S1). We understand that the proposed structures are just one example out of many candidates. The cluster structure also may not be similar to its crystal structure. However, we changed many simulation parameters to check the results; we conclude that a thickness of 40 nm is too thick for observing the clusters. Further studies and more involved calculations are necessary to comprehend the real structure of the clusters in this freestanding ultrathin film state.

To further confirm the effectiveness of the ultrathin freestanding film in observing the nanoscale structure of the ionic liquid and to verify the existence of well-ordered clusters in an ionic liquid as a general phenomenon, four other ionic liquids, **1**, bmimBF$_4$ (1-butyl-3-methylimidazolium tetrafluoroborate), **2**, omimBF$_4$ (1-methyl-3-octylimidazolium tetrafluoroborate), **3**, [emim][MDEGSO$_4$] (1-ethyl-3-methylimidazolium 2-(2-methoxyethoxy)ethylsulfate), and **4**, [AAim]TFSI (1,3-diallylimidazolium bis(trifluoromethanesulfonyl) imide), with melting points of −71, −80, −65, and −91.6 °C, respectively, were tested and viewed under HRTEM. Using the same experimental procedure, ionic liquids **1**−**4** were first diluted with acetonitrile to 0.10 wt %. Then the solutions were deposited onto the carbon nanotube grid to obtain the respective freestanding thin films. Well-ordered clusters could be observed in

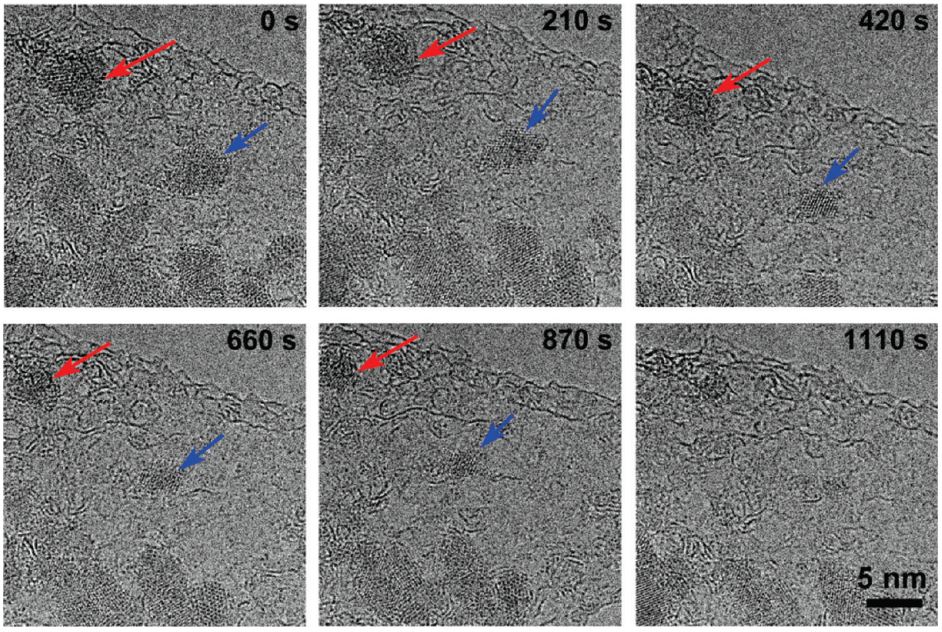

Figure 4. HRTEM images (observed at E = 120 kV, T = 300 °C) showing the dissociation of the clusters at high temperature under continuous electron beam radiation. The images were obtained over ca. 18 min (from top left to bottom right). The numbers shown at the top right corner of each image represent the time history of the observation in seconds. The red and blue arrows point to two isolated clusters, which degraded gradually.

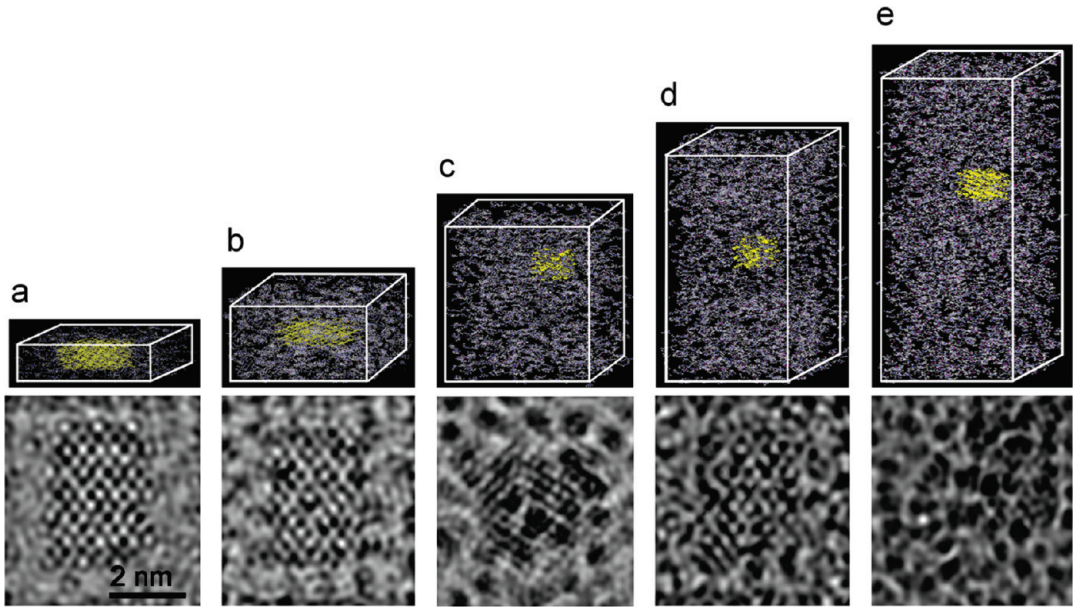

Figure 5. Five constructed models for bmiml clusters in the thin liquid films with a thickness of (a) 5 nm, (b) 10 nm, (c) 20 nm, (d) 30 nm, and (e) 40 nm. The yellow color highlights the location of the clusters. The corresponding simulated TEM images are present at the bottom of each model.

all four samples at room temperature (Figure S12), suggesting that this kind of spatial heterogeneity is common in the liquid phase of imidazolium-based ionic liquids. In addition, it is found that the cluster size is on the order of a few nanometers and might be proportional to the size of the composed ions of the ionic liquid, which is consistent with the former studies on the relationship between cluster size and alkyl chain length of some imidazolium-based ionic liquids.[25−27]

Figure 6a shows a series of representative HRTEM images of a bmiml thin film during *in situ* cooling in TEM. Isolated clusters are observed even at 0 and −40 °C. The cluster size distribution is shown in Figure 6b. The size distribution at 0 °C is almost the same as that at 25 °C (compare Figure 2d with Figure 6b). At −40 °C, we observed a bimodal distribution of clusters, which may be due to an interplay of the growth and coalescence of the clusters. At −60 °C, however, the

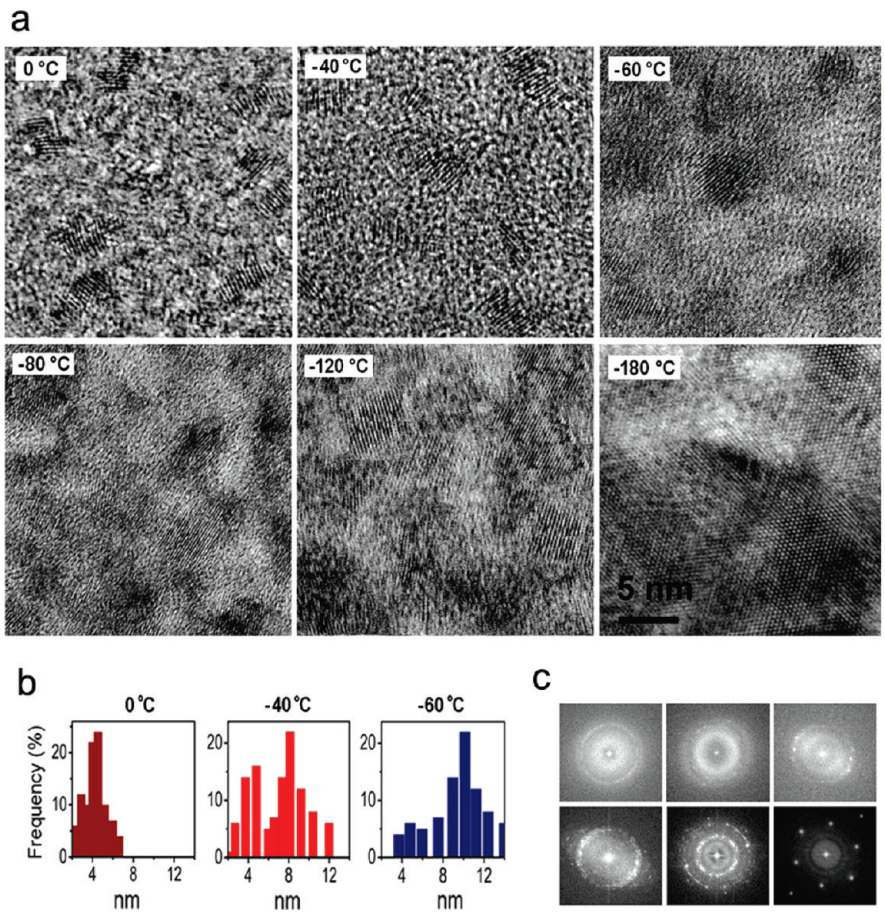

Figure 6. HRTEM images of the bmiml thin film upon temperature decrease. (a) HRTEM images of bmiml under different temperatures *via* an *in situ* cooling procedure (from 25 to −180 °C at a rate of −1 °C/min). (b) Histograms of cluster size distribution at 0, −40, and −60 °C; for each plot, we measured 80 to 110 clusters within the same area of 300 nm by 300 nm. (c) Corresponding fast Fourier transform (FFT) images of (a) showing the development of crystallinity during the temperature decrease (from top left to bottom right; the temperature for each FFT image is 0, −40, −60, −80, −120, and −180 °C, respectively). The indexing of FFT images obtained under −180 °C indicates the same features stemming from the crystal structure of bulk bmiml (Supporting Figure S13). Selected area electron diffraction patterns recorded under each temperature are presented in Supporting Figure S14.

distribution has a single peak centered around 10.2 nm, which is larger than those at 0 and −40 °C. Both the size and the number of clusters increase remarkably at this temperature, indicating the onset of the phase transition. The well-ordered clusters can always be observed down to −120 °C. From the viewpoint of the microstructure of bmiml, the crucial difference before and after the phase transition can solely be attributed to the size and density of the clusters, and the clusters act as seeds for bulk crystal formation. The corresponding fast Fourier transform (FFT) images (Figure 6c) and electron diffraction patterns at different temperatures (Supporting Figure S14) show clear evidence that ordered structures gradually form as the temperature decreases.

On the basis of the above observations, the size and mobility of the clusters determine the macroscopic properties of the ionic liquid. Due to the Coulombic interactions among the net charges of the ions as well as interactions among complex chemical groups,[17,28] the clusters in ionic liquids should be much more stable than those in water and other molecular liquids. From the HRTEM observations, the lifetime of the bmiml cluster is longer than several minutes, which could be due to an interfacial effect in the freestanding film. It is known that ionic liquids self-assemble at the liquid−vacuum interface.[29−31] Furthermore, recent studies on ionic liquid-based interfaces by photoelectron spectroscopy,[32,33] sum-frequency generation spectroscopy,[34] and *in situ* STM/AFM measurements[35] also suggested that a multilayer architecture or surface ordering and enrichment effects could occur at ionic liquid surfaces. These kinds of specific surface effects may play a key role in inducing and stabilizing the well-ordered clusters observed here. However, in the present system, the freestanding ionic liquid is free from a solid−liquid interface, and the gas−liquid interfacial layer also accounts for a very small proportion of the ultrathin film (see Supporting Information section 7). We believe that the freestanding thin film can be regarded as a part of the bulk liquid. At the same time we noted that the surface effect is important for the stabilization of the cluster, and enable us to capture the structures by HRTEM.

Temperature-dependent HRTEM studies have shown that the clusters can be observed in the whole range of liquid bmimI, indicating that the characteristic fluidity of ionic liquids is related to the diffusion of the clusters rather than the conventional molecular motions. This is consistent with a reported nonexponential dynamics and an unusually broad spectrum of dynamic processes of the ionic liquids,[17,36,37] which has never been observed in molecular liquids of comparable viscosity. During the phase transition process, as the size of the clusters increases to a critical extent, they tend to associate with each other to form larger clusters with less mobility, leading to a solid-like state.

CONCLUSIONS

In summary, we have observed the microstructure of ionic liquids by using HRTEM with the aid of a specially designed carbon nanotube grid to obtain an ultrathin freestanding film. The thickness of the as-obtained freestanding film is only several tens of nanometers, which ensures high-resolution imaging of the ionic liquid film by TEM. The cluster structure inside an imidazolium-based ionic liquid bmimI was directly observed for the first time. It was found that the bmimI clusters showed a high radiation and thermal stability based on our *in situ* TEM investigations and played an important role during the phase transition of bmimI, which indicated that the existence of clusters could be one of the intrinsic properties of many ionic liquids in its whole liquid phase range. HRTEM imaging of freestanding liquid films, as a building block of the bulk liquid, will provide new insights into the properties of liquids and further enable the exploration of liquid behavior in low-dimensional systems.

METHODS

High-purity grade bmimI ionic liquids were purchased from Merck KGaA (Darmstadt, Germany). The purity was checked by NMR spectroscopy and HPLC, and Karl Fischer titration confirmed the water content below 80 ppm. The influence of possible impurities (if any) in the bmimI sample has been safely ruled out by using thoroughly purified bmimI in our laboratory (Supporting Information, section 4). In a typical experiment, bmimI was first dissolved in acetonitrile (HPLC grade) at a concentrations of 0.10 wt %, and a drop of bmimI solution was spin-coated on the carbon nanotube grid. Then the grid was kept at 80 °C for 72 h under high vacuum (1×10^{-5} Pa) to remove acetonitrile. The typical area sizes of the holes on the carbon nanotube grid are larger than 500 nm^2, and we always focus on the center area of the liquid film to exclude the unfavorable interaction between the ionic liquid and the outer surface of the carbon nanotubes.

TEM observations, selected area electron diffraction (SAED), and energy dispersive X-ray (EDX) measurements were performed using a JEOL JEM-2010F/UHR microscope (equipped with a CEOS Cs corrector operating at 120 kV) and a JEM-2100F/HR (equipped with a superatmospheric thin-window X-ray detector operating at 80 kV). Temperature-dependent HRTEM experiments were performed by equipping the microscope with a heating holder (JEOL, model EM-21130) or cryo-holder (Gatan, model 626DH Cryo transfer system).

Acknowledgment. We thank S. Fan and K. Jiang (Tsinghua University) for supplying carbon naotube based TEM grids. This work was supported by Grants-in-Aid for Specific Area Research (No. 19084008) on Carbon Nanotube Nano-Electronics and for Scientific Research A (No.19205003) of MEXT, Japan. S.C. is grateful for the Postdoctoral Fellowship for Foreign Researchers of the Japan Society for Promotion of Science.

Supporting Information Available: A detailed description of the consideration of TEM observations of ionic liquid, electron beam radiation effects, interface effects, checking on impurities, a series of *in situ* TEM images, and corresponding movies showing the stability of the film and clusters under continuous beam radiation, as well as the analysis on FFT and electron diffraction patterns. This material is available free of charge *via* the Internet at http://pubs.acs.org.

REFERENCES AND NOTES

1. Ludwig, R. Water: From Clusters to the Bulk. *Angew. Chem., Int. Ed.* **2001**, *40*, 1808–1827.
2. Smith, J. D.; Cappa, C. D.; Wilson, K. R.; Cohen, R. C.; Geissler, P. L.; Saykally, R. J. Unified Description of Temperature-Dependent Hydrogen Bond Rearrangements in Liquid Water. *Proc. Natl. Acad. Sci. U. S. A.* **2005**, *102*, 14171–14174.
3. Gruenloh, C. J.; Carney, J. R.; Arrington, C. A.; Zwier, T. S.; Fredericks, S. Y.; Jordan, K. D. Infrared Spectrum of a Molecular Ice Cube: The S_4 and D_{2d} Water Octamers in Benzene-$(water)_8$. *Science* **1997**, *276*, 1678–1681.
4. Vaitheeswaran, S.; Yin, H.; Rasaiah, J. C.; Hummer, G. Water Clusters in Nonpolar Cavities. *Proc. Natl. Acad. Sci. U. S. A.* **2004**, *101*, 17002–17005.
5. Tamenori, Y.; Okada, K.; Takahashi, O.; Arakawa, S.; Tabayashi, K.; Hiraya, A.; Gejo, T.; Honma, K. Hydrogen Bonding in Methanol Clusters Probed by Inner-shell Photoabsorption Spectroscopy in the Carbon and Oxygen K-edge Regions. *J. Chem. Phys.* **2008**, *128*, 124321.
6. Denifl, S.; Zappa, F.; Mähr, I.; Mauacher, A.; Probst, M.; Märk, T. D.; Scheier, P. Inelastic Electron Interaction with Chloroform Clusters Embedded in Helium Droplets. *J. Am. Chem. Soc.* **2008**, *130*, 5065–5071.
7. Donnelly, S. E.; Birtcher, R. C.; Allen, C. W.; Morrison, I.; Furuya, K.; Song, M. H.; Mitsuishi, K.; Dahmen, U. Ordering in a Fluid Inert Gas Confined by Flat Surfaces. *Science* **2002**, *296*, 507–510.
8. Cao, B.; Starace, A. K.; Judd, O. H.; Jarrolda, M. F. Phase Coexistence in Melting Aluminum Clusters. *J. Chem. Phys.* **2009**, *130*, 204303.
9. Dermota, T. E.; Zhong, Q.; Castleman, A. W., Jr Ultrafast Dynamics in Cluster Systems. *Chem. Rev.* **2004**, *104*, 1861–1886.
10. Williamson, M. J.; Tromp, R. M.; Vereecken, P. M.; Hull, R.; Ross, F. M. Dynamic Microscopy of Nanoscale Cluster Growth at the Solid−Liquid Interface. *Nat. Mater.* **2003**, *2*, 532–536.
11. Zheng, H.; Smith, R. K.; Jun, Y.; Kisielowski, C.; Dahmen, U.; Alivisatos, A. P. Observation of Single Colloidal Platinum Nanocrystal Growth Trajectories. *Science* **2009**, *324*, 1309–1312.
12. Wasserscheid, P.; Welton, T., Eds. *Ionic Liquids in Synthesis*; Wiley-VCH: New York, 2003; pp 41−126.
13. Borra, E. F.; Seddiki, O.; Angel, R.; Eisenstein, D.; Hickson, P.; Seddon, K. R.; Worden, S. P. Deposition of Metal Films on an Ionic Liquid as a Basis for a Lunar Telescope. *Nature* **2007**, *447*, 979–981.
14. Rogers, R. D.; Seddon, K. R. Ionic Liquids−Solvents of the Future? *Science* **2003**, *302*, 792–793.
15. Smiglak, M.; Andreas Metlen, A.; Rogers, R. D. The Second Evolution of Ionic Liquids: From Solvents and Separations to Advanced Materials−Energetic Examples from the

Ionic Liquid Cookbook. *Acc. Chem. Res.* **2007**, *40*, 1182–1192.
16. Smith, E. F.; Villar Garcia, I. J.; Briggs, D.; Licence, P. Ionic Liquids in Vacuo; Solution-Phase X-ray Photoelectron Spectroscopy. *Chem. Commun.* **2005**, 5633–5635.
17. Weingrtner, H. Understanding Ionic Liquids at the Molecular Level: Facts, Problems, and Controversies. *Angew. Chem., Int. Ed.* **2008**, *47*, 654–670.
18. Triolo, A.; Russina, O.; Hans-Jurgen Bleif, H. J.; Cola, E. D. Nanoscale Segregation in Room Temperature Ionic Liquids. *J. Phys. Chem. B* **2007**, *111*, 4641–4644.
19. Del Pópolo, M. G.; Kohanoff, J.; Lynden-Bell, R. M.; Pinilla, C. Clusters, Liquids, and Crystals of Dialkyimidazolium Salts. A Combined Perspective from ab initio and Classical Computer Simulations. *Acc. Chem. Res.* **2007**, *40*, 1156–1164.
20. Iwata, K.; Okajima, H.; Saha, S.; Hamaguchi, H. Local Structure Formation in Alkyl-Imidazolium-Based Ionic Liquids as Revealed by Linear and Nonlinear Raman Spectroscopy. *Acc. Chem. Res.* **2007**, *40*, 1174–1181.
21. Zhang, L.; Feng, C.; Chen, Z.; Liu, L.; Jiang, K.; Li, Q.; Fan, S. Superaligned Carbon Nanotube Grid for High Resolution Transmission Electron Microscopy of Nanomaterials. *Nano Lett.* **2008**, *8*, 2564–2569.
22. Fukushima, T.; Kosaka, A.; Ishimura, Y.; Yamamoto, T.; Takigawa, T.; Ishii, N.; Aida, T. Molecular Ordering of Organic Molten Salts Triggered by Single-Walled Carbon Nanotubes. *Science* **2003**, *300*, 2072–2074.
23. Kirkland, E. J. *Advanced Computing in Electron Microscopy*; Plenum Publishing Corp.: New York, 1998.
24. Nakakoshi, M.; Shiro, M.; Fujimoto, T.; Machinami, T.; Seki, H.; Tashiro, M.; Nishikawa, K. Crystal Structure of 1-Butyl-3-Methylimidazolium Iodide. *Chem. Lett.* **2006**, *35*, 1400–1401.
25. Shigeto, S.; Hamaguchi, H. Evidence for Mesoscopic Local Structures in Ionic Liquids: CARS Signal Spatial Distribution of $C_n$mim[PF_6] (n=4,6,8). *Chem. Phys. Lett.* **2006**, *427*, 329–332.
26. Triolo, A.; Russina, O.; Bleif, H.; Di Cola, E. Nanoscale Segregation in Room Temperature Ionic Liquids. *J. Phys. Chem. B* **2007**, *111*, 4641–4644.
27. Lopes, J. N. C.; Pádua, A. A. H. Nanostructural Organization in Ionic Liquids. *J. Phys. Chem. B* **2006**, *110*, 3330–3335.
28. Castner, E. W.; Wishart, J. F.; Shirota, H. Intermolecular Dynamics, Interactions, and Solvation in Ionic Liquids. *Acc. Chem. Res.* **2007**, *40*, 1217–1227.
29. Bhargava, B. L.; Balasubramanian, S. Layering at an Ionic Liquid-Vapor Interface: A Molecular Dynamics Simulation Study of [bmim][PF_6]. *J. Am. Chem. Soc.* **2006**, *128*, 10073–10078.
30. Yan, T.; Li, S.; Jiang, W.; Gao, X.; Xiang, B.; Voth, G. A. Structure of the Liquid-Vacuum Interface of Room-Temperature Ionic Liquids: A Molecular Dynamics Study. *J. Phys. Chem. B* **2006**, *110*, 1800–1806.
31. Santos, C. S.; Baldelli, S. Gas-Liquid Interface of Room-Temperature Ionic Liquids. *Chem. Soc. Rev.* **2010**, *39*, 2136–2145.
32. Lovelock, K. R. J.; Villar-Garcia, I. J.; Maier, F.; Steinrück, H. P.; Licence, P. Photoelectron Spectroscopy of Ionic Liquid-Based Interfaces. *Chem. Rev.* **2010**, *110*, 5158–5190.
33. Maier, F.; Cremer, T.; Kolbeck, C.; Lovelock, K. R. J.; Paape, N.; Schulz, P. S.; Wasserscheid, P.; Steinrück, H. P. Insights into the Surface Composition and Enrichment Effects of Ionic Liquids and Ionic Liquid Mixtures. *Phys. Chem. Chem. Phys.* **2010**, *12*, 1905–1915.
34. Santos, C. S.; Rivera-Rubero, S.; Dibrov, S.; Baldelli, S. Ions at the Surface of a Room-Temperature Ionic Liquid. *J. Phys. Chem. C* **2007**, *111*, 7682–7691.
35. Hayes, R.; Warr, G. G.; Atkin, R. At the Interface: Solvation and Designing Ionic Liquids. *Phys. Chem. Chem. Phys.* **2010**, *12*, 1709–1723.
36. Xu, W.; Cooper, E. I.; Angell, C. A. Ionic Liquids: Ion Mobilities, Glass Temperatures, and Fragilities. *J. Phys. Chem. B* **2003**, *107*, 6170–6178.
37. Triolo, A. Thermodynamics, Structure, and Dynamics in Room Temperature Ionic Liquids: The Case of 1-Butyl-3-methyl Imidazolium Hexafluorophosphate ([bmim][PF_6]). *J. Phys. Chem. B* **2006**, *110*, 21357–21364.